

# Application of a New Approach for the Quantitation of Drug Synergism to the Combination of *cis*-Diamminedichloroplatinum and 1- $\beta$ -D-Arabinofuranosylcytosine<sup>1</sup>

William R. Greco,<sup>2</sup> Hyoung Sook Park, and Youcef M. Rustum

Grace Cancer Drug Center [W. R. G., H. S. P., Y. M. R.] and Department of Biomathematics [W. R. G.], Roswell Park Memorial Institute, New York State Department of Health, Buffalo, New York 14263

## ABSTRACT

This report describes the application of a new approach, the universal response surface approach, to the quantitative assessment of drug interaction, *i.e.*, the determination of synergism, antagonism, additivity, potentiation, inhibition, and coalitive action. The specific drug combination and experimental growth system for this introductory application was that of 1- $\beta$ -D-arabinofuranosylcytosine (ara-C) and cisplatin with simultaneous drug exposure (1, 3, 6, 12, or 48 h) against L1210 leukemia *in vitro*. To quantitate the type and degree of drug interaction, a model was fitted using nonlinear regression to the data from each separate experiment, and parameters were estimated (K. C. Syracuse and W. R. Greco, Proc. Biopharm. Sect. Am. Stat. Assoc., 127-132, 1986). The parameters included the maximum cell density over background in absence of drug, the background cell density in presence of infinite drug, the 50% inhibitory concentrations and concentration-effect slopes for each drug, and a synergism-antagonism parameter,  $\alpha$ . A positive  $\alpha$  indicates synergism, a negative  $\alpha$ , antagonism, and a zero  $\alpha$ , additivity. Maximal synergy was found with a 3-h exposure of ara-C + cisplatin, with  $\alpha = 3.08 \pm 0.96$  (SE) and  $2.44 \pm 0.70$  in two separate experiments. Four different graphic representations of the raw data and fitted curves provide visual indications of goodness of fit of the estimated dose-response surface to the data and visual indications of the intensity of drug interaction. The universal response surface approach is mathematically consistent with the traditional isobologram approach but is more objective, is more quantitative, and is more easily automated. Although specifically developed for *in vitro* cancer chemotherapy applications, the universal response surface approach should prove to be useful in the fields of pharmacology, toxicology, epidemiology, and biomedical science in general.

## INTRODUCTION

This report describes the application of a new approach, URSA,<sup>3</sup> to the quantitative assessment of drug interaction, *i.e.*, the determination of synergism, antagonism, additivity, potentiation, inhibition, and coalitive action. The specific drug combination-experimental system for this introductory application was that of ara-C and DDP against L1210 leukemia *in vitro*. This report describes in detail the analysis of data from one 48-h growth experiment which began with a 3-h incubation of

L1210 cells with various combinations of ara-C and DDP. In addition, this report briefly describes the results from 11 additional separate growth experiments, with incubation times ranging from 1 to 48 h and explores the dynamics (time course) of the synergistic interaction between DDP and ara-C. Since the emphasis of this report is on the new data analysis approach, discussion of the biomedical implications of the results is kept to a minimum. The biological and clinical implications of this study are only briefly described under "Discussion."

The situation which gave impetus to the development of this new approach for assessing drug interactions included: (a) the determination of synergism, antagonism, and additivity among drugs is widespread and important in biomedicine (over 20,000 articles in the biomedical literature from 1981 to 1988 used "synergism" as a key word, and of these, over 2400 were cancer related); (b) there is widespread disagreement over concepts and terminology; (c) there exist many different approaches for assessing drug interactions which will result in different conclusions for the same data set; (d) most older approaches include limitations; (e) conclusions regarding drug interactions are often suboptimally used.

Put more succinctly, quantitative drug interaction assessment is widely done, differently done, often poorly done, and yet important.

URSA was developed by adapting and combining elements from many well-established approaches for assessing drug interactions. The fundamental concept from Loewe (1) of isobolograms underpins the whole approach. Many of the equations and symbols were adapted from those of Chou and Talalay (2, 3). The guidelines for the derivation of drug interaction models were adapted from Berenbaum (4) but also share features of earlier work from Hewlett and Plackett (5, 6) and Finney (7). The statistical concept of generalized linear (or nonlinear) models by McCullagh and Nelder (8) provides URSA with its universal nature. Finally, the use of response surface techniques in assessing drug interactions has gained wide acceptance because of the work by Carter's group (9).

The general approach used in the present study to quantitate synergism has been reported previously (10-13), and the specific application to the data presented in this paper has been reported previously in an abstract (14). However, this is the first report of the application of URSA to real laboratory data published in a peer-reviewed journal. A brief description of the advantages of this method over traditional methods is included in the "Discussion"; a more extensive comparative critical review is in preparation. Mathematical derivations of drug interaction models are provided in Appendix 1. More extensive mathematical descriptions and statistical characterizations of the drug interaction models are included in a paper in the statistical literature (11). A brief description of the statistical approach, the mathematical models, and the derivation of the

Received 4/14/89; revised 2/28/90.

The costs of publication of this article were defrayed in part by the payment of page charges. This article must therefore be hereby marked *advertisement* in accordance with 18 U.S.C. Section 1734 solely to indicate this fact.

<sup>1</sup> Supported by National Cancer Institute Grants CA18420, CA50456, and CA46732.

<sup>2</sup> To whom requests for reprints should be addressed.

<sup>3</sup> The abbreviations used are: URSA, universal response surface approach; cisplatin or DDP, *cis*-diamminedichloroplatinum; ara-C, 1- $\beta$ -D-arabinofuranosylcytosine; 2-D, two-dimensional; 3-D, three-dimensional; PC, personal computer. Mathematical symbols used are:  $E$ , measured cell density; [DRUG], [ara-C], and [DDP], drug, ara-C, and cisplatin concentration respectively;  $E_{max}$ , maximum cell density over background at zero drug concentration;  $B$ , background cell density at infinite drug concentration;  $D_m$ ,  $ID_{50}$ , or  $IC_{50}$ , median effective concentration of drug or concentration of drug which inhibits growth ( $E_{max}$ ) by 50%;  $D_x$ ,  $ID_{10}$ , and  $ID_{90}$ , concentration of drug which inhibits growth ( $E_{max}$ ) by  $X\%$ , by 10%, and by 90%, respectively;  $D_{m,ara-C}$  and  $D_{m,DDP}$ , median effective concentration of ara-C and cisplatin;  $D_{x,ara-C}$ ,  $D_{x,DDP}$ , concentration of ara-C, DDP which inhibits growth ( $E_{max}$ ) by  $X\%$ ;  $m$ ,  $m_{ara-C}$ , and  $m_{DDP}$ , slope parameters for concentration-effect curves;  $\alpha$ , synergism-antagonism parameter;  $\gamma$ , interaction parameter for

**MATERIALS AND METHODS**

**Chemicals.** Cisplatin was obtained from the Bristol-Myers Company (Syracuse, NY). ara-C was supplied by Sigma Chemical Company (St. Louis, MO). The purity of the compounds was determined by high pressure liquid chromatography to be 98%. Drugs were dissolved and serial dilutions made in RPMI 1640 plus 20 mM 4-(2-hydroxyethyl)-1-piperazineethanesulfonic acid (Gibco, Buffalo, NY). Drug solutions were sterilized by passage through a 0.2- $\mu$ m Acrodisc from Gelman Sciences, Inc. (Ann Arbor, MI).

**Exposure of Cells.** Murine leukemia L1210 cells were grown in suspension culture in RPMI 1640 supplemented with 10% heat-inactivated fetal bovine serum and 20 mM 4-(2-hydroxyethyl)-1-piperazineethanesulfonic acid, pH 7.3, at 37°C. To assess drug effects on cell growth, L1210 cells in log phase with a doubling time of about 12 h were utilized. L1210 cells at a final concentration of 50,000 cells/ml in 4 ml of the above medium supplemented with 10% heat-inactivated fetal bovine serum (complete medium) were exposed to six logarithmically spaced concentrations of ara-C and cisplatin centered at the predicted ID<sub>50</sub> for each drug in a 6<sup>2</sup> factorial design, for a total of 36 different combinations. From 4 to 8 control (0  $\mu$ M ara-C plus 0  $\mu$ M DDP) tubes and 2 tubes of each of the other 35 drug combinations were used. Tubes were stoppered, randomly placed in racks, and incubated in an upright position at 37°C during the drug exposure (1–48 h) and the subsequent drug-free growth period. Drug exposure was followed by two washes with sterile 0.9% NaCl solution and final resuspension in complete medium (free of drug). Growth was determined by counting the number of cells in tubes with a Coulter electronic cell counter, Model ZBI (Coulter Electronics, Inc., Hialeah, FL) 48 h after the start of drug exposure.

**Data Analysis.** Equation 1 was fitted to the complete data set from an experiment (74–78 measurements) with unweighted least squares nonlinear regression, and parameters were estimated (10–14). Equation 1 contains the respective drug concentrations [ara-C] and [DDP] as inputs; and the measured cell density, *E*, as the output. The 7 estimable parameters include: *E*<sub>max</sub>, the maximum cell density, over background, at 0 drug concentration; *B*, the extrapolated background cell density in the presence of an infinite drug concentration; the respective ID<sub>50</sub>s or median effective concentrations, *D*<sub>m,ara-C</sub> and *D*<sub>m,DDP</sub>; the respective concentration-effect slopes, *m*<sub>ara-C</sub> and *m*<sub>DDP</sub>; and the synergism-antagonism parameter,  $\alpha$ . When  $\alpha$  is positive, synergism is indicated; when  $\alpha$  is negative, antagonism is indicated; and when  $\alpha$  is 0, no interaction or additivity is indicated.

$$1 = \frac{[\text{ara-C}]}{D_{m,\text{ara-C}} \left( \frac{E - B}{E_{\text{max}} - E + B} \right)^{1/m_{\text{ara-C}}} + \frac{[\text{DDP}]}{D_{m,\text{DDP}} \left( \frac{E - B}{E_{\text{max}} - E + B} \right)^{1/m_{\text{DDP}}}} + \frac{\alpha[\text{ara-C}][\text{DDP}]}{D_{m,\text{ara-C}} D_{m,\text{DDP}} \left( \frac{E - B}{E_{\text{max}} - E + B} \right)^{1/2m_{\text{ara-C}}} \left( \frac{E - B}{E_{\text{max}} - E + B} \right)^{1/2m_{\text{DDP}}}} \tag{1}$$

$$E = \frac{E_{\text{max}} \left( \frac{[\text{DRUG}]}{D_m} \right)^m}{1 + \left( \frac{[\text{DRUG}]}{D_m} \right)^m} + B \tag{2}$$

Equation 1 allows the slopes of the concentration-effect curves for the two drugs to be unequal. Equation 1 was derived (see "Appendix 1") using the guidelines of Berenbaum (4) for defining the predicted additivity surface for a combination when the concentration-effect models are known (or assumed) for each individual drug, but with the addition of a first order interaction term. A convention used in Equations 1 and 2, is that as drug concentration(s) increases, the measured response (cell density) decreases; the slope parameter, *m*, is negative. Equations 1 and 2 could be easily adapted so that the measured pharmacological effect (growth inhibition) would increase with increasing drug concentration.

The general sigmoid-*E*<sub>max</sub> or logistic equation (with a background

later shown) to be appropriate for both ara-C and DDP. The form of Equation 2 (without *B*) and with *f<sub>a</sub>* (fraction affected) = *E*/*E*<sub>max</sub>, is simply a rearrangement of the median-effect equation of Chou and Talalay (2, 3, 15) or of the Hill model (16–19). Also, the terms and symbols *D<sub>m</sub>* and *m* are from Ref. 2.

Equation 1 was fitted to data using custom software called SYNFIT, which was written in the computer language, MicroSoft C (MicroSoft Corp., Bellevue, WA). SYNFIT uses a version of the Marquardt algorithm (20) for nonlinear regression as described by Nash (21). The output of the program includes parameter estimates, asymptotic standard errors, 95% confidence limits for the parameters, and residual analyses. All comparisons for statistical significance were performed with a type I error rate of 0.05. Since Equation 1 is not in closed form, a one-dimensional bisection root finder (e.g., Ref. 22) was used to calculate predicted values of *E*. Initial parameter estimates for the *D<sub>m</sub>* and *m* parameters for the nonlinear regression were obtained by fitting the median-effect equation of Chou and Talalay (2) to the single drug data with weighted linear regression. The SAS/PC software package, Version 6 (23), was used to generate the 3-D graph of Fig. 1. The graphs in Figs. 2–4 were made by simulating data from Equation 1, using the estimated parameters from the best fit of Equation 1 to the observed data, with custom FORTRAN programs, and plotting the simulated data by hand. All software was run on IBM PC/AT, IBM PC/XT, and Leading Edge Model M microcomputers. Inquiries regarding distribution of the custom software package, SYNFIT, should be addressed to W. R. Greco.

URSA could be implemented with many commercial statistical software packages. We have used URSA with the mainframe version of BMDP (24), the PC version of SAS (23), and PCNONLIN (25). To be suitable for implementation of URSA, a package must include a nonlinear regression procedure which does not require the coding of analytical derivatives and, in order to code the root finder, does allow the function definition to include IF statements, and either GOTO statements and/or loops. An example of a set of model-definition statements for fitting Equation 1 to data is listed in Appendix 2. This example consists of control language for SAS and will be appropriate for SAS running on microcomputers, minicomputers, and mainframe computers. By adapting this example, interested researchers should be able to implement URSA into many other commercial statistical packages which include a nonlinear regression module.

We are implementing URSA into custom user-friendly software in C language for microcomputers running the MicroSoft Disk Operating System, instead of emphasizing the use of commercial software packages for several reasons: (a) many researchers may be unacquainted with the use of general nonlinear regression software; (b) researchers may be hesitant to spend several hundred dollars to purchase general statistical software for implementing a new approach to data analysis; (c) the most current concepts and approaches can be implemented into a custom software package, whereas commercial statistical packages may present limitations and restrictions; (d) custom software can be custom engineered for a specific use and audience, whereas general packages must accommodate wide areas of application.

**General Description of URSA.** An unambiguous, logical, and functional definition for the term, "synergism," is crucial before progress can be made in its assessment and good use can be made of its claim. An intuitive definition is that synergism occurs between two agents when the observed pharmacological effect (growth inhibition in this report) of a combination is more than what would be predicted from a good knowledge of the individual effects from each agent alone. A specific, complete, functional definition was provided above in the description of Equation 1, but a more general, succinct definition is provided here. Given specific, appropriate models for each agent alone, such as Equation 2, and given a logically derived model for the combination of the two agents which includes an interaction term with an estimable interaction parameter, such as  $\alpha$  in Equation 1; when the true interaction parameter is positive, synergism exists; when the true interaction parameter is negative, antagonism exists; and then the true interaction term is zero, no interaction (additivity) exists. To estimate the true interaction parameter, a combination model, such as Equation

approach, such as nonlinear regression, and the true parameter is estimated, along with a measure of uncertainty in the estimate. The word “potentiation” is reserved for the case in which one drug has no effect by itself, but increases the effect of an individually effective second drug; “inhibition” is reserved for the case in which one drug has no effect by itself but decreases the effect of a second drug, and “coalitive action” is reserved for the case in which two drugs have no effects by themselves, but the combination does have an effect. It should be noted here that there are many useful, functional definitions of synergism that are less restrictive: they do not require a particular mathematical model to describe the drug interaction; but rather, they require only that the observed effect of the combination be greater than that predicted from a specific, simpler noninteraction (additivity) model (e.g., Refs. 2, 4, 26–28). However, if an appropriate, full interaction model can be adequately fitted to data for a particular experimental system, then quantitative approaches which utilize this model should be superior to approaches which do not.

The full general universal response surface approach consists of eight steps: (a) the functional form of the individual concentration-effect models for each drug is characterized (e.g., median effect, median effect with a background, logistic, exponential, exponential with a shoulder, linear, etc.) from past experience, theoretical considerations, and preliminary data; (b) a logical model for the joint action of the drug combination is derived using an adaptation of the guidelines of Berenbaum (4). Briefly, with Berenbaum’s approach the isobol constraint equation

$$1 = \frac{D_1}{D_{m_1}} + \frac{D_2}{D_{m_2}}$$

is assumed to be correct, specific mathematical models for the individual drug concentration-effect curves are assumed to be correct, and a composite model for joint drug effect for the case of no interaction (additivity) is derived. An adaptation of this approach (See Appendices 1C and 1D) consists of deriving composite models for joint drug effect for the cases of interaction (synergism, antagonism), which include interaction parameters; (c) the experiment is designed; (d) the experiment is conducted; (e) this model is fit to the full data set by an appropriate curve-fitting technique (e.g., weighted nonlinear regression, maximum likelihood estimation, etc.) which takes into account the statistical nature of the data (e.g., continuous responses, binary responses, counts, etc.) and data variation; (f) the goodness of fit of the model to the data is assessed by examining the 95% confidence intervals around the parameter estimates and by visually assessing the concordance of the fitted surface to the observed data points; (g) if the fit is good, the model is accepted, parameter estimates along with measures of uncertainty in the estimates are reported, and conclusions are made; (h) if the fit is not good, logical changes are made to the model, and steps 5–7 (or possibly steps 3–7), are repeated. If no logical model can be found which adequately fits the full data set, a model is derived for additivity (no interaction) using the guidelines of Berenbaum (4), this model is fit to all of the single drug data, the combination data are superimposed upon the fitted surface, and departures from additivity are noted by visual inspection.

As shown in the “Discussion,” the above new approach is mathematically consistent with the traditional isobologram approach but is more objective, is more quantitative, and is more easily automated.

## RESULTS

The results of a 3-h simultaneous exposure of L1210 with ara-C plus DDP are shown in Figs. 1–4. Each of these four figures illustrates a different view of both the measured data and the concentration-effect surface estimated from fitting Equation 1 to the data. It should be emphasized that none of the curves shown in Figs. 1–4 are merely hand-drawn curves intended to connect data points; rather they are all curves simulated from the best fit of Equation 1 to the data.

estimated concentration-effect surface. The vertical or  $Z$  axis is the unnormalized measured cell density, and the  $X$  and  $Y$  axes are drug concentrations on a linear scale. Solid data points lie above the fitted surface, and open points lie below. Vertical lines are drawn from the data points to the fitted surface. Data points which would be hidden by the surface have been excluded from this figure. The parameter estimates  $\pm$  SE from the fit of Equation 1 to the data in Fig. 1 are:  $E_{max} = 176,000 \pm 7,500$  cells/ml;  $B = 20,000 \pm 7,500$  cells/ml;  $D_{m,ara-C} = 14.6 \pm 1.8 \mu\text{M}$ ,  $m_{ara-C} = -0.916 \pm 0.010$ ;  $D_{m,DDP} = 9.81 \pm 0.87 \mu\text{M}$ ;  $m_{DDP} = -1.58 \pm 0.21$ ; and  $\alpha = 3.08 \pm 0.96$ . The 95% confidence interval for  $\alpha$  is from 1.14 to 5.02. Since this interval does not encompass 0, one can conclude that synergism between ara-C and DDP was demonstrated in this experiment. The 95% confidence interval for  $m_{ara-C}$  is  $-0.936$  to  $-0.896$ ; that for  $m_{DDP}$  is  $-2.00$  to  $-1.16$ . Since these intervals do not overlap, one can conclude that the concentration-effect curve for DDP is steeper than for ara-C; the individual concentration-effect curves are not parallel. The 95% confidence intervals for  $D_{m,ara-C}$  is from 11.0 to 18.2  $\mu\text{M}$ ; that for  $D_{m,DDP}$  is 8.05 to 11.6  $\mu\text{M}$ . Since the intervals overlap, one cannot conclude that DDP is more potent than ara-C under the specified experimental conditions.

The estimated background cell density (in the presence of an infinite drug concentration), 20,000 cells/ml, is reasonably close to but less than the seeded number of cells, 50,000 cells/ml. Both the death and the disintegration of cells caused by high concentrations of drugs and artifacts caused by washing and clumping may account for the fact that  $B$  is less than the seeded 50,000 cells/ml. This background can be noted in Fig. 1 as the height of the surface at the highest concentrations of drugs, 50  $\mu\text{M}$  ara-C plus 20  $\mu\text{M}$  DDP. The background parameter could have been better characterized if higher concentrations had been used. The  $E_{max}$  parameter represents the difference in cell density resulting from an exposure of cells to 0  $\mu\text{M}$

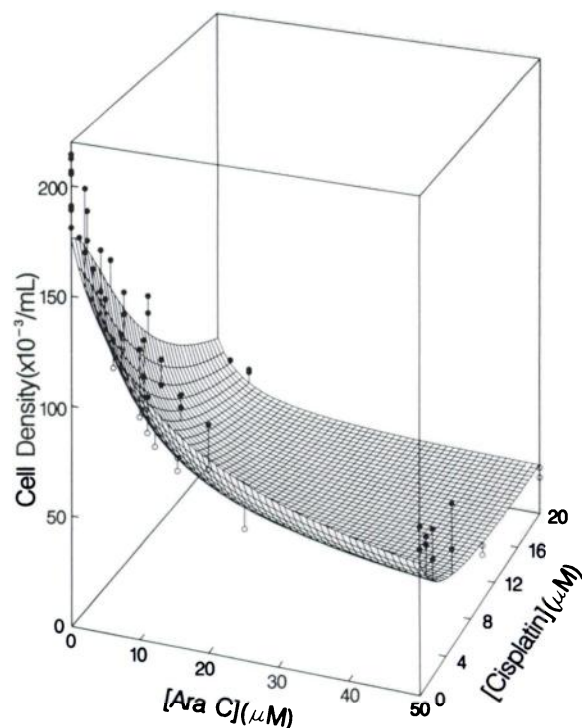


Fig. 1. Three-dimensional concentration-effect surface for a 3-h drug exposure to ara-C plus DDP. *Fishnet surface*, predicted concentration-effect surface, estimated from fitting Equation 1 to the data with nonlinear regression as described in the text; *points*, measured cell densities from single tubes. *Solid points* (●) are

Fig. 2. Families of 2-dimensional concentration-effect curves for a 3-h drug exposure to ara-C and DDP. The curves are predicted concentration-effect curves, estimated as described in Fig. 1 and in the text. This set of curves is a 2-dimensional representation of the 3-dimensional surface in Fig. 1, but with the ordinate transformed to a percentage of  $[E_{max} + B]$ . Points, transformed measured cell densities.

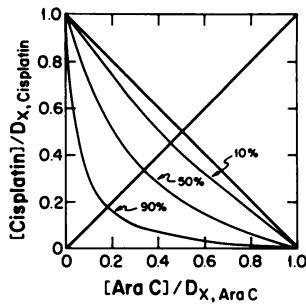
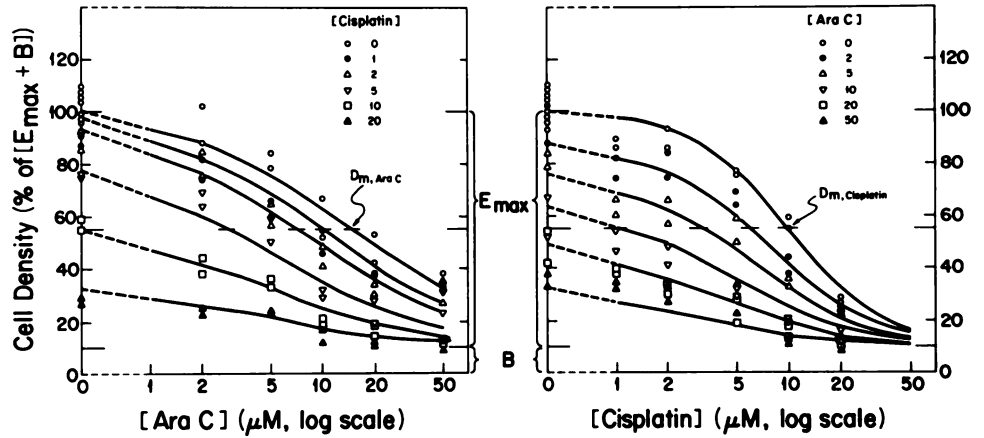


Fig. 3. Families of two-dimensional isobols for a 3-h drug exposure to ara-C and DDP. The curves were estimated as described in Fig. 1 and in the text. The set of isobol contours is another 2-dimensional representation of the 3-dimensional surface in Fig. 1, but with the ara-C and DDP concentrations transformed by division by the appropriate  $D_x$  value.

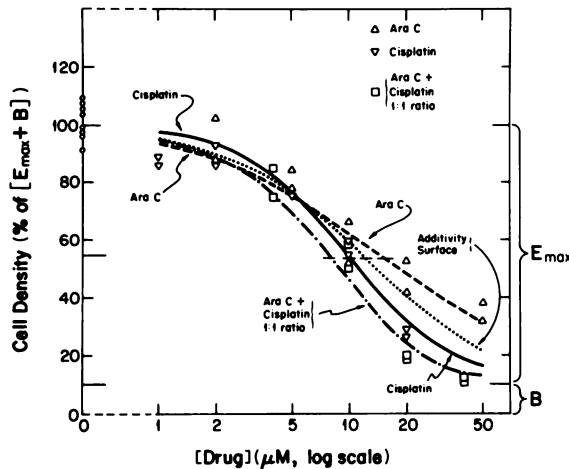


Fig. 4. Predicted concentration-effect curves for 3-h drug exposure to ara-C alone, to DDP alone, to ara-C plus DDP in a 1:1 ratio, and to ara-C plus DDP in a 1:1 ratio which would show no interaction (additivity). The curves were simulated as described in Figs. 1-3 and in the text. This set of curves is yet another informative 2-dimensional representation of the 3-dimensional surface in Fig. 1. Points, transformed measured cell densities.

ara-C plus 0  $\mu\text{M}$  DDP versus infinite ara-C plus infinite DDP. Or, in other words,  $E_{max}$  is the range of response that can be affected by drugs. The sum of  $E_{max}$  plus  $B$  is the estimated cell density at 0  $\mu\text{M}$  ara-C plus 0  $\mu\text{M}$  DDP. The estimated median effective concentrations  $D_{m,ara-C}$  and  $D_{m,DDP}$  are those concentrations necessary to reduce  $E_{max}$  (not the sum of  $E_{max} + B$ ) by 50%. Negative slope parameters of concentration-effect curves would indicate inhibitory drugs, e.g.,  $m_{ara-C}$  and  $m_{DDP}$  in this study, whereas positive slope parameters indicate stimulatory

Talalay (2), who use a positive slope for both inhibitory and stimulatory drugs. A larger absolute value of the slope parameter results in a steeper concentration-effect curve. Although for the experiment shown in Fig. 1, the estimated  $m_{DDP}$  is 1.7-fold greater than  $m_{ara-C}$ , slope differences are not clearly seen in the 3-D plot of Fig. 1. Since the synergism-antagonism parameter,  $\alpha$ , is positive, synergism is indicated. The magnitude of  $\alpha$ , 3.08, is reasonably large, but like the difference in slopes, is difficult to appreciate from Fig. 1. Thus, although the 3-D concentration-effect surface in Fig. 1 provides a good overall picture, Figs. 2-4 which are three different 2-D representations of the results of the same experiment, are necessary to provide visual indications of goodness of fit of the estimated surface to the data and visual indications of the intensity of drug interaction.

Fig. 2 consists of two sets of families of 2-D concentration-effect curves. The same raw data are shown in both the left and right panels. The curves are sections of the best fit surface estimated from the fit of Equation 1 to the data. In fact, the left set of six curves are transformations of slices of the full surface depicted in Fig. 1, expressed as a percentage of the predicted control  $[E_{max} + B]$ , from the face of the cube nearest the viewer, and continuing through five higher DDP levels. Analogously, the right panel of Fig. 2 could be constructed as transformations of slices of the surface in Fig. 1, starting at the left face, and continuing toward the right face at five higher ara-C levels. Note that the concentration scales in Fig. 2 are logarithmic. Note also that the predicted effect at 0  $\mu\text{M}$  ara-C plus 0  $\mu\text{M}$  DDP is normalized to 100%. In Fig. 2, the relative magnitude of  $E_{max}$  and  $B$  can be seen. The estimated  $D_m$  values are designated by horizontal bars. Note that the  $D_m$  (or  $ID_{50}$ ) does not appear at the 50% level, but rather at the midpoint of the  $E_{max}$  range. It is clear that DDP has the steeper sloping concentration-effect curves. The goodness-of-fit of the data by the fitted surface can be visually assessed in Fig. 2 (29). The points are reasonably close to the fitted surface and reasonably random about the surface. Note that if each of 12 curves in Fig. 2 were simply drawn by hand to connect the points, the figure would appear quite different. However, like Fig. 1, Fig. 2 lacks a good visual impression of the degree of interaction between ara-C and DDP.

Fig. 3 is a 2-D isobolographic representation of the 3-D surface in Fig. 1. Isoeffect contours are shown at 10, 50, and 90% pharmacological effect, corresponding to cell densities of 178,400, 108,000, and 37,600 cells/ml, respectively. Note:

$$\% \text{ of pharmacological effect} = 100 \left[ \frac{[E - B]}{E_{max} - B} \right]$$

The diagonal line from the upper left to the lower right is the line of no interaction (additivity). No observed data points are shown because none appeared at exactly 10, 50, or 90% effect. The *ordinate* and *abscissa* are drug concentrations normalized by the respective  $D_x$  values ( $D_{10}$ ,  $D_{50}$ ,  $D_{90}$  values; estimated concentration resulting in  $X\%$  inhibition; e.g., 10, 50, 90% inhibition). The 3 curves in Fig. 3 are slices of Fig. 1 obtained by coming down from the top face of the cube, cutting at the 10, 50, and 90% levels (of  $E_{max}$ , not  $[E_{max} + B]$ ), and normalizing by the respective  $D_x$  values. The degree of bowing of the isobol contours is a visual indication of the degree of synergism. It should be emphasized that the curves in Fig. 3 are sections of the fitted concentration-effect surface and not handdrawn isobols derived from handdrawn concentration-effect curves (27). Note that all of the isobols in Fig. 3 are smooth and symmetrical (any roughness in the curves is due to the difficulty of drawing the curves from simulated data), even though  $m_{ara-C} \neq m_{DDP}$ . There have been many suggested geometric indices of the degree of bowing of an isobol (6). The synergism-antagonism parameter,  $\alpha$ , is algebraically related to these indices. For example, if the distance between the origin (0, 0) and the crossing of the diagonals (0.5, 0.5) is designated as  $ON$ , and the distance between the origin and the point where the rising (left to right) diagonal meets the 50% isobol is designated as  $OM$ , then the ratio  $S$  ( $S = ON/OM$ ), will be an index of synergism. A large ratio will indicate a lot of bowing and a large synergism. This ratio,  $S$ , is related to  $\alpha$  by Equation 3. The derivation of Equation 3 is included in Appendix 1C.

$$\alpha = 4(S^2 - S) \tag{3}$$

Note that for  $\alpha = 3.08$ , as in the present study,  $S = 1.51$ . This could be verified by the interested reader by using a ruler to measure the required distances in Fig. 3 and then making the required calculations. A form for the general isobol equation can be derived from Equation 1 by setting

$$E = [1 - 0.01X]E_{max} + B$$

and

$$D_m = D_x \left( \frac{X}{100 - X} \right)^{1/m}$$

(from Equation 2) and substituting these expressions in Equation 1. After some algebra, Equation 4, a general equation for an isobologram, results.

$$\frac{[DDP]}{D_{x,DDP}} = \frac{1 - \frac{[ara-C]}{D_{x,ara-C}}}{1 + \frac{\alpha[ara-C]}{D_{x,ara-C}} \left[ \frac{100 - X}{X} \right]^{(1/2m_1 + 1/2m_2)}} \tag{4}$$

Equation 4 is an hyperbola. It is the equation which describes the curves in Fig. 3. Note that at the  $ID_{50}$ , where  $E = 0.5E_{max} + B$ , the term

$$\frac{100 - X}{X}$$

raised to the power

$$\frac{1}{2m_1} + \frac{1}{2m_2}$$

becomes 1 and thus disappears from Equation 4. Also, it is this

percentage effects. In Fig. 3 the 90% isobol is more bowed than the 50% isobol, which is more bowed than the 10% isobol. Also note that  $\alpha$  in Equation 4 also effects the degree of bowing, i.e., as a positive  $\alpha$  increases, the degree of bowing will increase.

Although the isobol representation does give a visual indication of the degree of interaction, it lacks two main desirable features: (a) raw data cannot be superimposed on the fitted curve to provide a visual measure of goodness of fit; and (b) a good indication of the vertical distance between the synergism surface and the predicted additivity surface is not provided. While Fig. 2 includes the first feature, Fig. 4 includes both of these features. Fig. 4 is another 2-D representation of Fig. 1. The layout of the axes of Fig. 4 is the same as that of Fig. 2. Four concentrations-effect curves are included in Fig. 4: *Curve 1*, ara-C alone; *Curve 2*, DDP alone; *Curve 3*, ara-C plus DDP in a 1:1 ratio; and *Curve 4*, the predicted additivity curve for ara-C plus DDP in a 1:1 ratio. The first 3 curves are appropriate slices through the full concentration-effect surface of Fig. 1. Corresponding raw data are superimposed on the 3 curves. The fourth curve was simulated with Equation 1 after setting  $\alpha = 0$ . It is clearly evident from Fig. 4 that DDP has a steeper concentration-effect curve than does ara-C. The additivity curve for a 1:1 concentration ratio of ara-C plus DDP lies between the respective curves for ara-C and DDP. The fitted curve for the 1:1 ratio lies below and to the left of the other 3 curves. The estimated  $D_m$  values for the four curves are: *Curve 1*, ara-C alone, 14.6  $\mu\text{M}$ ; *Curve 2*, DDP alone; 9.81  $\mu\text{M}$ ; *Curve 3*, ara-C plus DDP in a 1:1 ratio, 7.86  $\mu\text{M}$  (or 3.93  $\mu\text{M}$  concentrations of each drug); and *Curve 4*, additivity curve of ara-C plus DDP in a 1:1 ratio, 10.6  $\mu\text{M}$  (or 5.28  $\mu\text{M}$  concentrations of each drug). Two logical measures of synergistic effect would include the horizontal distance between *Curves 3* and *4* at the median effect, 2.74  $\mu\text{M}$ , and the ratio of  $D_m$  values for *Curves 3* and *4*, 1.35. Note that this ratio, 1.35, is not the same as the ratio  $S$ , 1.51 calculated from the isobol representation of Fig. 3. Other logical measures of synergistic effect include: horizontal differences and ratios at other effect levels; the maximum horizontal difference and maximum ratio; vertical differences and ratios at various drug levels; and the maximum vertical difference and maximum ratio.

A total of 12 individual experiments were performed, 3 with a 1-h drug exposure time, 2 with 3 h, 2 with 6 h, 2 with 12 h, and 3 with 48 h exposure, each with a 74-78-tube design.

Fig. 5 illustrates the effect of drug exposure time on the  $\alpha$  parameter estimated by fitting Equation 1 to the data sets from the 12 separate experiments. The plotted points in Fig. 5 are displaced slightly from the true exposure times to allow a visual comparison of the 95% confidence intervals from repeat experiments. There is a suggestion of a pattern to the time course of synergism in Fig. 1. Mild synergism occurs at a 1-h drug exposure, synergism seems to peak at 3-6 h, and then synergism becomes mild again from 6 to 48 h drug exposure. However, because the 95% confidence intervals for  $\alpha$  all overlap and because the number of experiments conducted at the suggested peak interval of synergism for drug exposure (3-6 h) was small, and because one of the experiments conducted with a 6-h drug exposure showed enhanced synergism while one did not, more experiments will have to be conducted in the range of 1-12 h drug exposure time to conclusively characterize the time course of synergism.

## DISCUSSION

The present study is the first report of a specific application

# Explore Litigation Insights

Docket Alarm provides insights to develop a more informed litigation strategy and the peace of mind of knowing you're on top of things.

## Real-Time Litigation Alerts



Keep your litigation team up-to-date with **real-time alerts** and advanced team management tools built for the enterprise, all while greatly reducing PACER spend.

Our comprehensive service means we can handle Federal, State, and Administrative courts across the country.

## Advanced Docket Research



With over 230 million records, Docket Alarm's cloud-native docket research platform finds what other services can't. Coverage includes Federal, State, plus PTAB, TTAB, ITC and NLRB decisions, all in one place.

Identify arguments that have been successful in the past with full text, pinpoint searching. Link to case law cited within any court document via Fastcase.

## Analytics At Your Fingertips



Learn what happened the last time a particular judge, opposing counsel or company faced cases similar to yours.

Advanced out-of-the-box PTAB and TTAB analytics are always at your fingertips.

## API

Docket Alarm offers a powerful API (application programming interface) to developers that want to integrate case filings into their apps.

## LAW FIRMS

Build custom dashboards for your attorneys and clients with live data direct from the court.

Automate many repetitive legal tasks like conflict checks, document management, and marketing.

## FINANCIAL INSTITUTIONS

Litigation and bankruptcy checks for companies and debtors.

## E-DISCOVERY AND LEGAL VENDORS

Sync your system to PACER to automate legal marketing.